S12-004

ATP synthase dynamics and tentoxin binding probed using hybrid bacterial/chloroplast enzyme assemblies

R Hein[1], WC Tucker[1,2], Z Du[2], T Levine[3], K Kuczera[1], G Haran[3], Z Gromet-Elhanan[2] and ML Richter[1]

[1]*Department of Molecular Biosciences, The University of Kansas, Lawrence KS 66045 USA.* markl@ukans.edu

[2]*Department of Biological Chemistry and* [3]*Chemical Physics Department, Weizmann Institute of Science, Rehovot 76100, Israel, 972-8-9344118. z.gromet-elhanan@weizmann.ac.il*

Keywords: Chloroplast, ATP synthase, tentoxin, rotational catalysis

Introduction

The photosynthetic F_OF_1 ATP synthase couples the movement of protons down an electrochemical proton gradient to the synthesis of ATP. The enzyme is composed of a membrane-spanning proton channel (F_O) and a peripheral membrane sector (F_1) which contains the catalytic sites for reversible ATP synthesis. The catalytic F_1 portion is comprised of five different polypeptide subunits designated α to ε in order of decreasing molecular weight with a stoichiometry of $\alpha_3\beta_3\gamma_1\delta_1\varepsilon_1$. Three catalytic sites, located primarily on the β subunits at αβ subunit interfaces, interconvert between three different conformational states during ATP synthesis via energy-dependent affinity changes in substrate binding and product release (Boyer, 1997). Several recent studies of bacterial F_1 (Noji et al., 1997; Omote et al., 1999) and F_OF_1 (Sambongi et al., 1999; Panke et al., 2000) have suggested that this may be achieved by rotation of the γ subunit relative to the $\alpha_3\beta_3$ sub-assembly. Until now, rotational catalysis has not been convincingly demonstrated for the photosynthetic enzyme.

Tentoxin, a cyclic tetrapeptide [cyclo L-leucyl-N-methyl-methyl-(z)-dehydro-phenylalanyl-glycyl-N-methyl-alanyl], produced by phytopathogenic fungi from the *Alternaria* genus, acts as a highly specific, uncompetetive inhibitor with respect to nucleotide substrates, of the chloroplast ATP synthase (Steele et al., 1976;1978). Binding of one molecule of tentoxin to a high affinity (K_d <10^{-8} M) site on chloroplast F_1 (CF_1) results in almost total inhibition of its ATPase activity, most likely by blocking the cooperative release of nucleotides during the catalytic cycle (Hu et al., 1993; Santolini et al., 1999). Further binding of tentoxin to one (Santolini et al., 1999) or two (Mochimaru & Sakurai, 1997) lower affinity (K_d >10^{-6} M) sites on CF_1 reactivates and actually stimulates the inhibited enzyme by an unknown mechanism. Similarly, low concentrations of tentoxin inhibit ATP synthesis by thylakoid membranes and higher concentrations partially restore ATP synthesis activity (Sigalat et al., 1995).

Avni et al. (1992) identified a correlation between tentoxin sensitivities of different *Nicotiana* species and the type of amino acid residue present at position 83 in the β amino acid sequence. Species with aspartate in this position were tentoxin sensitive whereas those with glutamic acid were tentoxin resistant. Moreover, mutation of Glu^{83} to Asp^{83} in the β subunit of tentoxin-resistant *Chlamydomonas reinhardtii* induced tentoxin sensitivity in that organism (Avni et al., 1992; Hu et al., 1997). This work has led to the identification of a cleft

at the catalytic interface of the N-terminal domains of the α and β subunits which is the likely binding site for tentoxin (Tucker et al., 2001b).

We have constructed hybrid enzymes in which cloned α, β and γ subunits from photosynthetic bacteria and from spinach chloroplasts were assembled into two different functional core $\alpha_3\beta_3\gamma$ ATPases (Du et al., 2001; Tucker et al., 2001b). In this communication we describe studies which have utilized this system to a) identify essential features of the tentoxin binding interaction using site-directed mutagenesis, and b) show that the hybrid photosynthetic enzyme is capable of rotary catalysis.

Materials and methods

Hybrid enzyme assemblies.

Two types of assembled hybrids were prepared. One contained the $\alpha^{(R)}$ subunit of the F_1 of *Rhodospirillum rubrum* (RrF_1) and the $\beta^{(C)}$ and $\gamma^{(C)}$ subunits of spinach CF_1. The presence of Asp^{83} enabled this hybrid to undergo stimulation but not inhibition by tentoxin (Tucker te al., 2001a). Three separate mutations at specific sites in the $\alpha^{(R)}$ subunits were prepared using inverse PCR (Sokolov et al., 1999). An $\alpha^{(R)K132P}$ mutation was constructed by enzymatic amplification of the expression plasmid pET3a-$RrF_1\alpha$ described previously (Tucker et al., 2001a). Two additional point mutations, $\alpha^{(R)Y292A}$ and $\alpha^{(R)R304Q}$, were constructed using the expression plasmid pET3a-$RrF_1\alpha^{M2}$ which encodes a chimeric $\alpha^{(R)}$ subunit containing the sequence of the RrF_1 α except for a short segment (127 to 133) corresponding to the spinach CF_1 α (Tucker et al., 2001b). These mutants were checked for appearance of tentoxin inhibition as well as stimulation (see results B). The second hybrid enzyme, that was used for rotational studies (see results C) was composed of $\alpha^{(R)}{}_3\beta^{(R)}{}_3\gamma^{(C)}$ and showed much higher ATPase activity than the $\alpha^{(R)}{}_3\beta^{(C)}{}_3\gamma^{(C)}$ hybrid (Du et al., 2001; Tucker et al., 2001b). Nucleotides encoding six histidine residues were incorporated at the 5' end of its $\alpha^{(R)}$ gene. All mutations were confirmed by sequencing the entire modified α gene using the fluorescent dideoxy method (Averboukh et al., 1996). Washed inclusion bodies containing the expressed *wild-type* (wt) or mutant proteins were prepared from *E. coli* cells, folded and assembled using the single-step dialysis procedure and gel purification described by Du et al. (2001) and Tucker et al. (2001a).

Docking simulations.

A molecular dynamics trajectory of the dominant A conformer of tentoxin was generated using the NMR-derived values for dihedral angles (Pinet et al., 1995). Atomic partial charges were assigned to tentoxin following the Gasteiger and Marsili methods using SYBYL (Tripos, Inc., St. Louis, MO). A homology model of CF_1 prepared using the coordinates from the MF_1 crystal structure (Abrahams et al., 1994) was kindly provided by Dr. Seigfried Engelbrecht. Quanta was used to restrict all complete residues within a 20 Å radius of the βAsp^{83} in the homology modeled CF_1. This process was repeated for each of the three β subunits. SYBYL was used to add all essential hydrogens, and atomic partial charges were assigned from the Kollman-united atom set to each of the Quanta generated spheres. The water molecules present in the homology model were removed from the sphere coordinate files to eliminate possible interference with the docking simulation. Docking simulations were conducted with AutoDock 3.0 (Morris et al., 1998) using the Lamarckian genetic algorithm. Each docking simulation involved 50 LGA runs, each starting with 50 copies of the ligand placed on the grid. The interaction of a probe group, corresponding to each type of atom found in the ligand, with the αβ residues in the 20 Å sphere was computed on a 60x60x60 Å cubic grid

with 0.375 Å spacing centered in the active site. The grids are used as look-up tables for the evaluation of interaction energies (Goodsell & Olson, 1990) which are simulations of a distance-derived potential energy and an electrostatic addition for all ligand atoms plus the internal ligand energy.

Rotational Assays.

The hybrid $\alpha^{(R)}{}_3\beta^{(R)}{}_3\gamma^{(C)}$ containing the His tagged $\alpha^{(R)}$ subunit and $\gamma^{(C)}$ subunit biotinylated at its specific disulfide sulfhydryls was immobilized onto a flow cell as described in detail elsewhere (Noji et al., 1997). Rotation of a biotinylated fluorescent actin filament attached to this hybrid assembly via streptavidin was initiated by adding rotation buffer containing 50 mM Tricine-NaOH (ph 8), 4 mM $CaCl_2$ and 4 mM ATP and followed as described by Noji et al. (1997).

Results and discussion

Docking tentoxin into the binding cleft.

The three potential tentoxin binding clefts in CF_1 $\alpha_3\beta_3\gamma$ are located in the N-terminal domains of the α and β subunits at the three catalytic site interfaces. Small sections of two of the interfacial regions which contain the tentoxin binding cleft are shown in Figure 1. The catalytic nucleotide binding sites are located approximately 30 Å below the tentoxin binding cleft (not shown). Docking simulations were conducted using the major A conformer of tentoxin (Pinet et al., 1995). The AutoDock program identified multiple alternate docked orientations and binding energies for tentoxin in each of the three binding clefts. The program further associated similar orientations into clusters and ranked them based on free energy of binding. The lowest energy orientation for each site was chosen from the clusters with the greatest population. Remarkably, the simulations revealed significant structural differences among the three $\alpha\beta$ interfaces within the tentoxin binding clefts, and also large differences in the likely orientation of bound tentoxin. The greatest contrast was seen between the $\alpha^E\beta^E$ and $\alpha^T\beta^T$ pairs (Figure 1) which correspond to the pair forming the empty catalytic site and the pair with the catalytic site occupied by the ATP analog AMPPNP respectively, as designated for the mitochondrial F_1 (Abrahams et al., 1994).

In the $\alpha^E\beta^E$ cleft, tentoxin binds such that the ring axis is roughly parallel to the surface of the cleft. In this position tentoxin interacts with the stretch of residues between 127 and 133 on the α subunit shown in white in Figure 1, and also with βAsp^{83}, shown in yellow, both of which are known to be involved in conferring sensitivity to tentoxin inhibition (Avni et al., 1992; Tucker et al., 2001b). In the $\alpha^T\beta^T$ site, tentoxin assumes a very different conformation in which the axis of the ring is perpendicular to the protein surface and tentoxin is buried deeply within a gap between the α and β subunits. In this orientation tentoxin is inserted between βAsp^{83} and αArg^{304} (shown in cyan in Fig.1) which have been proposed to form a salt link in CF_1 (Groth & Pohl, 2001). The gap is absent in the $\alpha^E\beta^E$ cleft where βAsp^{83} and αArg^{304} are much closer to each other and much more likely to form a salt link. In the $\alpha^T\beta^T$ cleft, tentoxin does not interact with residues 127 to 133. Since these residues have been shown to affect inhibition but not stimulation, it is possible that the tentoxin orientation seen in the $\alpha^T\beta^T$ cleft is that which causes stimulation of catalytic activity as opposed to the orientation in the $\alpha^E\beta^E$ cleft which would instead be responsible for inhibition.

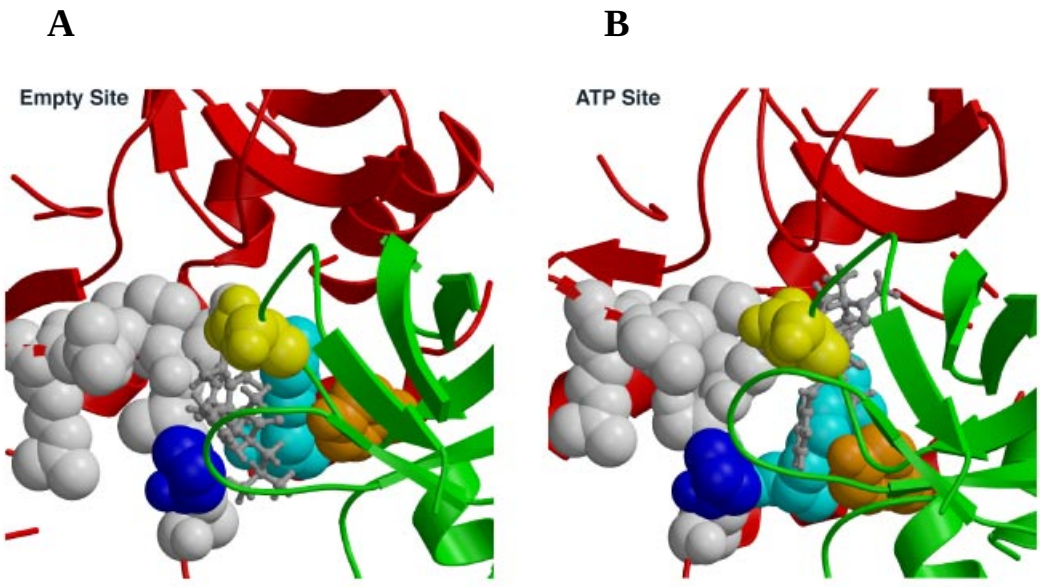

Figure 1. Models of the tentoxin binding clefts at the $\alpha^{E}\beta^{E}$ (A) and $\alpha^{T}\beta^{T}$ (B) interfaces. The α subunits are shown in red ribbons, β subunits in green ribbons. Space-filled residues: βAsp83, yellow; αArg304, cyan; α residues 127-133, white; αPro132, blue; αTyr292, orange. Tentoxin is modeled in ball-and-stick in gray.

B. The effects of mutations within the tentoxin binding cleft. Three different mutant α subunits were constructed to test specific features of the model shown in Figure 1 using the hybrid $\alpha^{(R)}{}_3\beta^{(C)}{}_3\gamma^{(C)}$. In the $\alpha^{(R)M2}$ chimera, seven amino acids (127-133, see Fig.1) from the CF_1 α were exchanged for the equivalent seven residues in the RrF_1 α. The exchange transformed the enzyme from one which is insensitive to inhibition to one which is inhibited by tentoxin (Tucker et al., 2001b). Of the seven residues, the one at position 132 is the only one that correlates well with tentoxin sensitivity when sequences from tentoxin sensitive and insensitive species are compared. Proline is present in this position in all tentoxin sensitive species whereas a lysine residue is present in this position in the RrF_1 α. It could be argued that the bulkier side chain of lysine interferes with entry of tentoxin into the binding cleft (Fig.1). However, the hybrid enzyme containing only the $\alpha^{(R)K132P}$ mutant remained insensitive to tentoxin, discounting this possibility (Table 1). It is likely, therefore, that more than one, and possibly all seven, of the amino acids between 127 and 133 are required to create the appropriate binding surface for tentoxin.

In a second mutation, Tyr^{292} (shown in orange in Fig.1) which has been proposed (Santolini et al., 1999) to Pi-stack with the phenyl ring of tentoxin was changed to alanine in the M2 α chimera. The substitution had no effect on the inhibitory or stimulatory action of tentoxin (Table 1) suggesting that this residue is not directly involved in tentoxin binding. In the third mutation, the potential of αArg^{304} to form a salt link with βAsp^{83} was assessed by changing αArg^{304} to glutamine. Indeed this substitution eliminated both the inhibitory and stimulatory effects of tentoxin (Table 1). Thus both βAsp^{83} and αArg^{304} are required for the inhibitory and stimulatory effects of tentoxin, possibly by setting up the appropriate conformation of the binding cleft as suggested by Groth and Pohl (2001). Since both residues are also required for the stimulatory action of tentoxin, it is possible that a salt link between these residues is initially required for entry of tentoxin into both inhibitory and stimulatory sites but once tentoxin has gained entry into the different clefts it assumes a different orientation depending

on the type of nucleotide bound at the respective catalytic site. For example, once it has gained entry into the stimulatory site tentoxin might insert itself between αArg^{304} and βAsp^{83} to assume the conformation shown in Figure 1B. This could block salt link formation which may lock the enzyme into an activated conformation..

Table 1. Sensitivity of hybrid $\alpha^{(R)}{}_3\beta^{(C)}{}_3\gamma^{(C)}$ assemblies containing various mutant $\alpha^{-R)}$ to tentoxin inhibition and stimulation

α subunit[1]	ATP hydrolysis activity (Percent of wild type)	Sensitivity to Tentoxin	
		Inhibition	Stimulation
—	100	-	+
wt,K132P	147	-	+
M2	172	+	+
M2,Y292A	106	+	+
M2,R304Q	125	-	-

[1]Wild-type or chimeric (M2) α subunits with the indicated mutations were assembled with the chloroplast β and γ subunits as described in the *Materials and Methods*. Mg^{2+}-dependent ATP hydrolysis was measured in the presence or absence of either 4 μM (inhibitory) or 200 μM (stimulatory) tentoxin (Tucker et al., 2001b).

C. Rotational studies. Preliminary experiments were undertaken to utilize the recombinant hybrid system to examine the propensity of the γ subunit of the photosynthetic ATP synthase to rotate as has been shown for two different non-photosynthetic bacterial enzymes. These experiments essentially duplicated those of Noji et al. (1997) in which a fluorescent actin filament of length between 1 and 2 μm was attached to the γ subunit of a thermophylic bacterial $\alpha_3\beta_3\gamma$ assembly which was bound to the surface of a nickel-coated glass cover slip via poly-histidine tags attached to the N-termini of the β subunits. The experiments departed from the bacterial ones in that the poly-histidine tags were attached to the N-termini of the α rather than β subunits and the actin filaments were attached to the disulfide sulfhydryls of the chloroplast γ subunit rather than to a specially engineered cysteine in the γ subunit as was the case in the bacterial system (Noji et al., 1997).

Approximately one in every hundred fluorescent actin filaments was observed to undergo continuous rotation in an anti-clockwise direction in the presence of CaATP as shown for a single filament in Figure 2. Rotation lasted for several minutes at rates between 0.5 and 2 rotations per second. The results clearly demonstrate the propensity of the photosynthetic enzyme to undergo rotational catalysis. The fact that the rotation is driven by CaATP is novel, and we are currently investigating its implications for rotational catalysis.

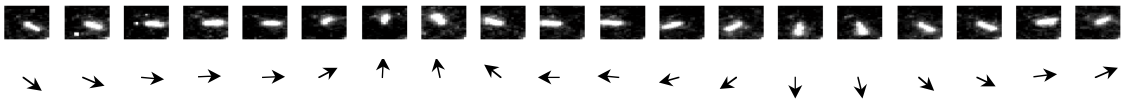

Figure 2. CaATP-dependent rotation of an actin filament attached to the γ subunit of **the $\alpha_3\beta_3\gamma$ assembly.** Each frame is a snapshot of a 2 μm actin filament attached to the disulfide sulfhydryls of the γ subunit. The sequence is from left to right with 60 ms between frames. The actin filament rotates in a counterclockwise direction.

References

Abrahams JP, Leslie AGW, Lutter R, Walker JE (1994) *Nature* 370, 621-628.

Averboukh L, Douglas SA, Zhao S, Lowe K, Mahler J, Pardee AB (1996) *Biotechniques* **20**, 918-921.

Avni A, Anderson JD, Holland N, Rochaix JD, Gromet-Elhanan Z, Edelman M (1992) *Science* **257**, 1245-1247.

Boyer PD (1997) *Annual Reviews of Biochemistry* **66**, 717-749.

Chen Z, Wu I., Richter ML, Gegenheimer PA (1992) *FEBS Letters* **298**, 69-73.

Du Z, Tucker WC, Richter ML, Gromet-Elhanan Z (2001) *Journal of Biological Chemistry* **276**, 11517-11523.

Goodsell GS, Olson AJ (1990) *Protein Structure and Functional Genetics* **8**, 195-204.

Groth G, Pohl E (2001) *Journal of Biological Chemistry* **276**, 1345-1352.

Hu N, Mills DA, Huchzermeyer B, Richter ML (1993) *Journal of Biological Chemistry* **268**, 8536-8540.

Hu D, Fiedler HR, Golan T, Edelman M, Strotmann H, Shavit N, Leu S (1997) *Journal of Biological Chemistry* **272**, 5457-5463.

Mochimaru M, Sakurai H (1997) *FEBS Letters* **419**, 23-26.

Morris GM,Goodsell GS, Hallisay RS, Huey R, Hart WE, Belew RK, Olsen AJ (1998) *Journal of Computational Chemistry* **19**, 1639-1662.

Noji H, Yasuda R, Yoshida M, Kinisita K (1997) *Nature* **386**, 299-302.

Omote H, Sambonmatsu N, Saito K, Sambongi Y, Iwamoto-Kihara A, Yanagida T, Wada Y, Futai M (1999) *Proceedings of the National Academy of Science USA* **96**, 7780-7784.

Panke O, Gumbiowski K, Junge W, Engelbrecht S (2000) *FEBS Letters* **472**, 34-38.

Pinet E, Neumann J, Dahse I, Girault G, Andrè F (1995) *Biopolymers* **36**, 135-152.

Sambongi Y, Iko Y, Tanabe M, Omote H, Iwamoto-Kihara A, Ueda I, Yanagida T, Wada Y, Futai M (1999) *Science* **286**, 1722-1724.

Santolini J, Haraux F, Sigalat C, moal G, Andrè F (1999) *Journal of Biological Chemistry* **274**, 849-858.

Sigalat C, Pitard B, Haraux F (1995) *FEBS Letters* **368**, 253-256.

Sokolov M, Lu L, Tucker W, Gao F, Gegenheimer PA, Richter ML (1999) *Journal of Biological Chemistry* **274**, 13524-13829.

Steele JA, Uchytil TF, Durbin RD, Bhatnagar P, Rich DH (1976) *Proceedings of the National Academy of Science USA* **73**, 2245-2248.

Steele JA, Durbin RD, Uchytil TF, Rich DH (1978) *Biochimica et Biophysica Acta* **501**, 78-82.

Tucker WC, Du Z, Hein R, Gromet-Elhanan Z, Richter ML (2001a) *European Journal of Biochemistry* **268**, 2179-2186.

Tucker WC, Du Z, Hein R, Gromet-Elhanan Z, Richter ML (2001b) *Biochemistry* **40**, 7542-7548.